LANGMUIR

pubs.acs.org/Langmuir Article

Maximizing Conversion of Surface Click Reactions for Versatile Molecular Modification on Metal Oxide Nanowires

Rimon Yamaguchi, Takuro Hosomi,* Masaya Otani, Kazuki Nagashima, Tsunaki Takahashi, Guozhu Zhang, Masaki Kanai, Hiroshi Masai, Jun Terao, and Takeshi Yanagida*

Cite This: *Langmuir* 2021, 37, 5172−5179 Read Online

ACCESS | Metrics & More | Article Recommendations | Supporting Information

ABSTRACT: Click reactions (e.g., Huisgen cycloaddition) on metal oxide nanostructures offer a versatile and robust surface molecular modification for various applications because they form strong covalent bonds in a wide range of molecular substrates. This study reports a rational strategy to maximize the conversion rate of surface click reactions on single-crystalline ZnO nanowires by monitoring the reaction progress. p-Polarized multiple-angle incidence resolution spectrometry (pMAIRS) and Fourier-transformed infrared (FT-IR) spectroscopy were employed to monitor the reaction progress of an azide-terminated self-assembled monolayer (SAM) on single-crystalline ZnO nanowires. Although various reaction parameters including the concentration of Cu(I) catalysts, triazolyl ligands, solvents, and target alkynes were systematically examined for the surface click reactions, 10−30% of terminal azide on the nanowire surface remained unreacted. Temperature-dependent FT-IR measurements revealed that such unreacted residual azides deteriorate the thermal stability of the nanowire molecular layer. To overcome this observed conversion limitation of click reactions on nanostructure surfaces, we considered the steric hindrance around the closely packed SAM reaction points, then experimented with dispersing the azide moiety into a methyl-terminated SAM. The mixed-SAM method significantly improved the azide conversion rate to almost 100%. This reaction method enables the construction of spatially patterned molecular surface modifications on metal oxide nanowire arrays without detrimental unreacted azide groups.

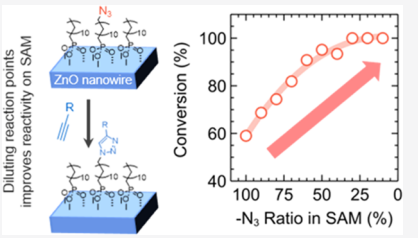

INTRODUCTION

Surface molecular modifications on metal oxide nanostructures have proven useful and exhibit potential to tailor physical and chemical properties for various applications, including electric, catalytic, and sensory devices.[1−5] The modifying organic compounds possess fine tunability and designability at the molecular level, qualities not attainable with bulk metal oxides.[2] Among various methodologies for such surface molecular modifications on metal oxide nanostructures, click reaction-based methods are particularly promising because of the strong covalent bonds formed and the wide range of usable compounds.[2−10] It has been reported that various functional molecules can be introduced via Huisgen cycloaddition with terminal azide or alkynyl groups on the top of self-assembled monolayers (SAMs).[11−15] This two-step surface molecular modification is complicated and different from conventional solution processes.[15] It is because fixations of reaction points (e.g., azide) on the surface increase their planar densities and limit their degree of freedom of translational motions, which can significantly affect their reactivities.[16,17] Therefore, the Huisgen cycloaddition reactivities on surfaces need to be monitored and investigated independently from those in the solutions. Some techniques to observe molecular changes like cyclic voltammetry,[13,15,18] or X-ray photoelectron spectroscopy[3,13,19,20] have successfully employed to monitor surface click reactions. Among them, infrared (IR) spectroscopy[4,6,13,15,19−21] are particularly useful because of the wide range of detectable functional groups. However, despite the superiority of IR spectroscopy, a comprehensive study on a single metal oxide nanostructured surfaces, exhaustively covering orientations and conformations of the molecular layers, steric environments around the reaction sites, effects of catalytic systems, optimized conditions to maximize conversions of the reaction sites, and the range of available substrates has not been investigated.

We recently reported that single crystal metal oxide nanowire arrays provide favorable surface for IR measurements.[22,23] A single-crystal metal oxide nanowire array consist of large amount of thin single crystals (diameters: 10−100 nm) perpendicularly grown on a flat substrate, which is favorable to investigate surface molecular quantities, configurations, and orientations by IR. We conducted time-dependent monitoring of the surface Huisgen reaction on a ZnO nanowire array and examined the effects of solution composition, additional ligands, and species of substrates. As a result, we found that

Received: January 12, 2021
Revised: April 1, 2021
Published: April 23, 2021

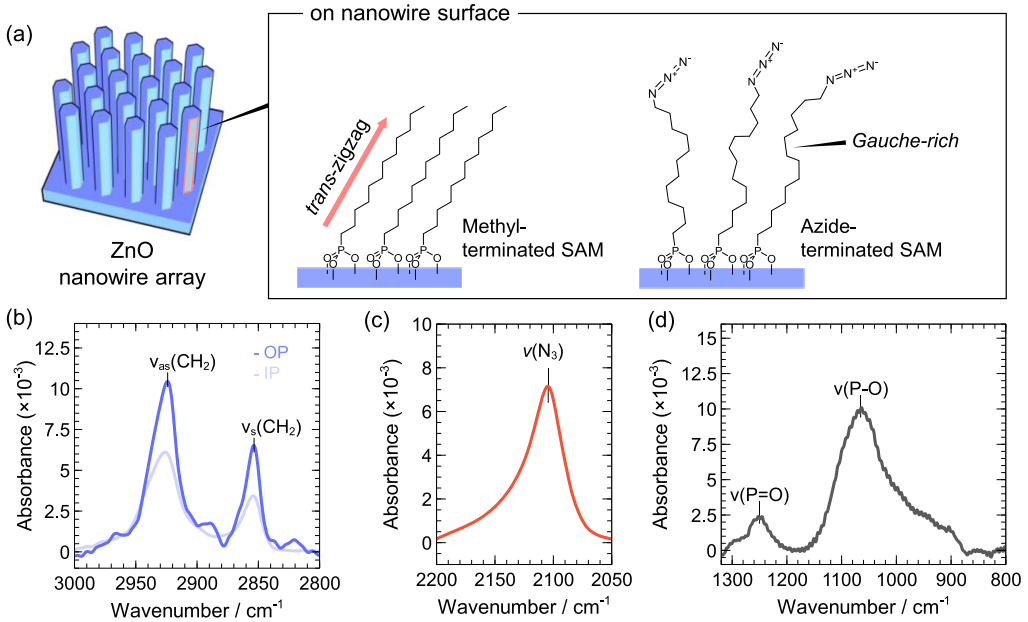

Figure 1. Conformational and spatial environments of terminal azide of the SAM on the ZnO nanowire arrays: (a) Scheme images of the alkyl conformation of the azide-terminated SAM on the ZnO nanowires; (b) pMAIRS spectrum of alkyl region (3000−2800 cm^{-1}) of azide-terminated SAM on the ZnO nanowire array (OP: out-of-plane signal, IP: in-plane signal); (c) FT-IR spectrum of azide region (2200−2050 cm^{-1}) and (d) phosphonic acid region (1300−800 cm^{-1}) of azide-terminated SAM on the ZnO nanowire array.

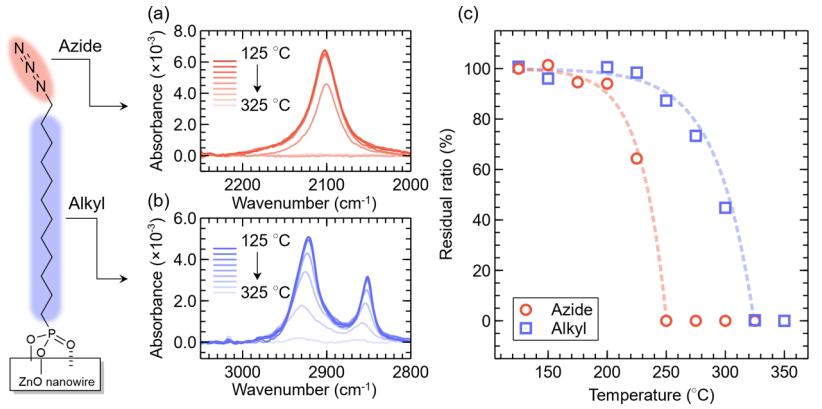

Figure 2. Thermal resistance of azide group on a SAM: temperature-dependent FT-IR spectra of (12-azidododecyl)phosphonic acid in the region of alkyl (a) and azide (b); (c) residual ratio of alkyl or azide calculated from IR peak area plotted against temperature.

(1) to obtain stable SAMs, high terminal azide conversion is preferable because of the thermal vulnerability of azides; (2) azide conversion rates do not reach 100% on completely azide-terminated SAMs even under optimized conditions; and (3) the use of mixed SAMs is effective in achieving stoichiometric azide conversion on the metal oxide nanowires. Based on these findings, we developed reaction conditions applicable to a wide range of target molecules on nanowire arrays.

RESULTS AND DISCUSSION

First, we evaluated the structural properties of the azide-terminated SAMs on ZnO nanowires (Figure S1), because the steric and electric environment of the reaction points significantly affect the reaction progress (Figure 1). Figure 1c,d show the Fourier-transformed infrared (FT-IR) spectrum of a ZnO nanowire array functionalized with (12-azidododecyl)phosphonic acid. The sharp azide absorption (at 2103 cm^{-1}) and the broad P−O absorption (centered at 1080 cm^{-1}) confirm the presence of the substrate on the nanowire surface. The P−O−H bands at 1000−920 cm^{-1} are almost absent, suggesting that the organic moieties stack on the ZnO surface via P−O−Zn bonds formed by dehydrative condensation between phosphonic acid and ZnO.[24,25] The binding structure is considered to be dominantly tridentate because only a small P═O absorption (around 1200−1250 cm^{-1}) is observed.[24] These characteristics are similar to those of methyl-terminated phosphonic acids on ZnO.[24,26,27] On the other hand, the behaviors of the alkyl chains of the (12-azidododecyl)phosphonic acid SAM are quite different from those of methyl-terminated SAMs. Figure 1b shows the p-polarized multiple-angle incidence resolution spectrometry (pMAIRS) spectra of the SAM alkyl region (OP: out-of-plane signal, IP: in-plane signal). Wavenumbers of the characteristic alkyl peaks ($\nu_{as}(CH_2)$: 2922 cm^{-1}, $\nu_s(CH_2)$: 2852 cm^{-1}) suggest that the SAM has a gauche-rich conformation, unlike typical methyl-terminated *n*-alkyl SAMs, which have trans-zigzag-dominated conformations. The average tilt angle was calculated to be almost perpendicular (86°) against the

https://doi.org/10.1021/acs.langmuir.1c00106
Langmuir 2021, 37, 5172−5179

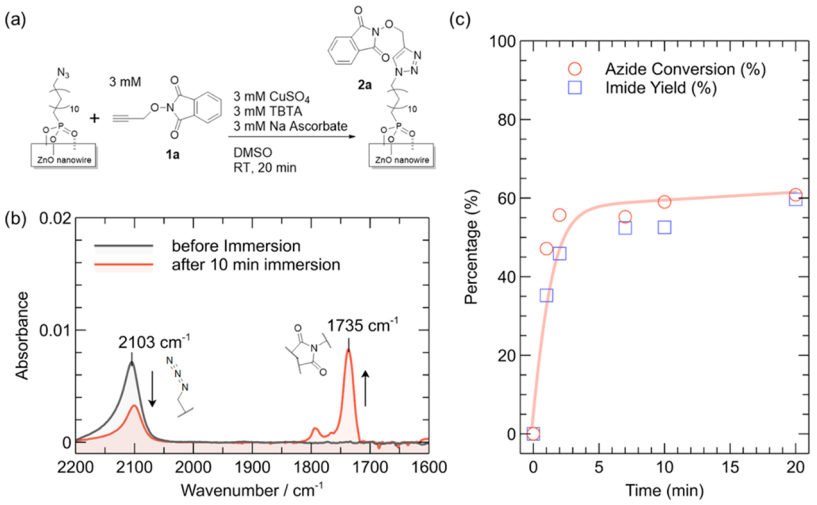

Figure 3. Scheme and spectroscopic trace of Huisgen cycloaddition on ZnO nanowires: (a) reaction scheme; (b) FT-IR spectral changes in the azide and imide regions, which show azide decrease and imide appearance via Huisgen cycloaddition; (c) azide conversion and imide yield of the Huisgen cycloaddition plotted against reaction time. The conversion and the yield are calculated against the initial azide amount on the SAM.

nanowire major axis by the ratio of OP and IP signal intensities,[28] indicating interfered alkyl chain orientations. These results suggest that the terminal azides make alkyl chain packing disordered (Figure 1a). It can be caused by the intermolecular azide-azide interactions[19] or steric hinderances by the terminal azides, which is relatively freely rotational and has larger rotational diameters compared with alkyl moieties. From these observations, the reaction points on the azide-terminated SAM are considered to exist in a spatially proximate environment.

We next examined the stability of the azide-terminated SAM, because the azide group is known for thermal instability derived from decomposition into N_2.[29] Such decompositions may lead to unintentional changes in the properties of the molecular-modified nanowires. To evaluate the thermal resistance of the azide group, we collected temperature-dependent FT-IR spectra of the azide-terminated SAM on ZnO nanowires (Figure 2). We observed that the alkyl peaks tolerated heat until the temperature reached approximately 250 °C, then gradually decreased between 250 and 300 °C. This result is consistent with previous stability research on simple alkyl monolayers.[30] In contrast, the azide absorption essentially disappears at approximately 200 °C, presumably as the azide undergoes thermal decomposition into N_2. Therefore, it can be said that residual azides can make the resultant molecular modifications instable by their unintentional decompositions. It will be especially problematic in some electric devices which are sensitive to the existence of polar functional groups like azides. In other words, full conversion of surface azides in the subsequent Huisgen cycloaddition reactions is crucial to achieve long-term, thermally robust monolayer surfaces.

To trace surface azide conversions, we conducted in situ FT-IR measurements during the Huisgen cycloaddition between the azide-terminated SAM and an alkyne in the presence of $CuSO_4$, sodium ascorbate, and tris(benzyltriazolylmethyl)-amine (TBTA). *N*-(2-Propynyl)phthalimide (**1a**) was chosen as the model substrate because of its FT-IR traceability derived from the imide moiety (Figure 3a). Figure 3b shows the FT-IR spectra of the SAM-modified ZnO nanowire before and after Huisgen cycloaddition for 10 min. The disappearance of the azide peak (2103 cm^{-1}) shows that the azide moiety is consumed by the reaction. Instead, the imide peak (1735 cm^{-1}) appeared after the reaction, showing the successful introduction of the imide moiety. Figure 2c shows the conversion rate of azide and yield of imide plotted against the reaction time (see Figure S2 for the raw spectra). These two values are consistent with each other, suggesting that the reaction proceeds without significant side reactions in that time. Interestingly, the reaction rate and azide conversion rate immediately saturated at a moderate yield, in contrast to typical Huisgen reaction behaviors in solution phases.[31] Such immediate saturations of conversion rates are also observed in the aliphatic or aromatic alkynes (Figure S3). Therefore, we next examined whether the conditions of the reaction can improve this limitation.

The conditions, concentrations, catalysts, ligands, and solvents of this reaction were screened. Conditions of each entry are shown in Table 1. First, both Cu(I) ions and ligands are necessary to this reaction. Almost no reaction proceeded without catalyst (entry 2) and without ligand (entry 3). The issue may be that Cu(I), which is thought to be an active species in the Huisgen reaction, is unstable even in the presence of sodium ascorbate.[32] In other words, the comparably slow solid−liquid reaction rate may reflect the instability of the active species. Therefore, we next investigated the effect of ligands, because certain kinds of diamine-type ligands are well known to be effective in stabilizing Cu(I) species by chelate effects.[33] The addition of (triazolylmethyl)-amine ligands improved the reaction progress (entries 4−7). In particular, (triazolylmethyl)amine, which has more than two triazolyl moieties (BBTA and TBTA), showed a significant effect, in contrast to the ineffectiveness of the MBTA. These trends also support the importance of the chelate effect of BBTA and TBTA for stabilization of Cu(I) species. Although BBTA yields higher yield than TBTA in the 3 mM condition, significantly decreased yield was observed in the lower concentration (0.3 mM) condition (entry 7). The changes of the solutions are also not effective to improve the yield and conversion (entries 8 and 9; see Figures S4 and S5 for detailed spectral changes). Therefore, we next examined the scope of the substrates under the reaction conditions because changes in the steric or electric structures of substrates may improve

https://doi.org/10.1021/acs.langmuir.1c00106
Langmuir 2021, 37, 5172−5179

Table 1. Entries of Reaction Conditions

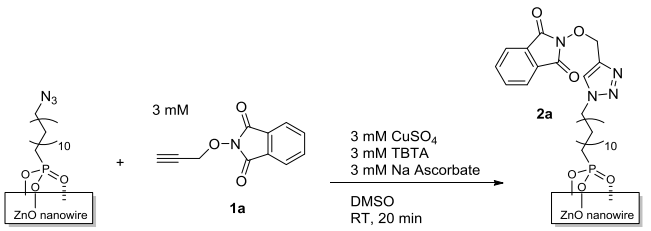

entry	conditions	-N_3 conv. (%)	**2a** yield (%)
1	none	61	60
2	without Cu(II) and ligand	0	0
3[a]	without ligand	6	<5
4	MBTA instead of TBTA	15	6
5	BBTA instead of TBTA	73	81
6	0.3 mM $CuSO_4$ and TBTA	24	32
7[a]	0.3 mM $CuSO_4$ and BBTA	7	<5
8[b]	DMF instead of DMSO	56	57
9	PEG400 instead of DMSO	57	51

[a] The small peak of the **2a** was buried in ambient water peaks due to the low yield (>5%).
[b] The reaction was stopped in 10 min to suppress dissolution of ZnO by amines generated by DMF decomposition.

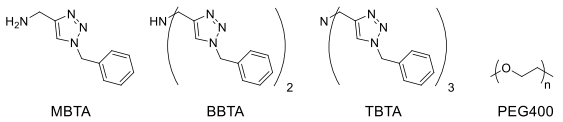

the azide conversion dramatically. We tested 16 kinds of alkynes (**1a**−**1p**), which contain a wide variety of alkynes with various sizes and functional groups. The spectral changes for each alkyne are shown in Figures S6−S8, and calculated azide conversions are summarized in Table 2. As can be seen in Table 2, these substrates show moderate conversion rates, excepting **1i**, which have carboxylic acid moiety. The low conversion of **1i** is considered to be a salt formation with TBTA to prevent the coordination ability to Cu(I). Repeated measurements (5 times) for a model substrate (**1e**) shows a standard error = 2.1%, indicating that our system has sufficient repeatability. From the above-mentioned entries, it can be said that the reaction conditions can be applicable to a wide range of substrates. However, even in the case of most reactive alkynes, the conversion rate saturates before 100%. In order to achieve full conversion of surface azides, another approach is still required.

Therefore, we developed a surface Huisgen reaction system that can realize almost 100% conversion of surface azide. We hypothesized that the limitation of the azide conversion described above are results of the close proximity of the terminal azides on the SAM. Once the triazole products are formed on the SAM surface, they are expected to act as steric hindrances which prevent copper-alkyne complexes from accessing the adjacent azides because each azide group is placed near to cause disordering of the alkyl chains as mentioned in Figure 1. This assumption is also supported by the negative relationships between the sizes of alkynes and azide conversion rates (Figure S9). Based on this assumption, we utilized the mixed-SAM method, which disperses (12-azidododecyl)phosphonic acid throughout a methyl-terminated dodecyl phosphonic acid (i.e., *n*-dodecyl phosphonic acid) SAM. Previous studies have shown the effectiveness of the mixed-SAM method.[29] Because the alkyl chain length in these two phosphonic acids is the same, the azide-terminated molecules can be considered well-dispersed in the dodecyl phosphonic acid SAM, and the azide moieties in the mixed SAM can be considered isolated. The wavenumber of $\nu_s(CH_2)$ first decreases with decrease of terminal azides ratio, and then saturates at the ratio is approximately 0.5 (Figure S10). This data suggests the uniform azide dispersion in the mixed SAM because the wavenumber of $\nu_s(CH_2)$ should decrease linearly if azide- and proton-terminated molecules form separated domains in the mixed SAM. The wavenumber of Figure 4 shows the transformed azide ratio against the initial azide amount (red line), and imide-functionalized ratio (blue line) for all phosphonic acids. The imide-functionalized ratio decreases by increase in the ratio of *n*-dodecyl phosphonic acid because reaction points (azide) in the SAM decreases. As can be seen, an increase in the ratio of *n*-dodecyl phosphonic acid causes a corresponding increase in the conversion. The azide conversion rate reaches almost 100% before the imide-functionalized ratio initiate significant decrease (>60%). This phenomenon strongly supports our hypothesis that the reacted molecules interfere the reactions of neighboring azides. These results clearly demonstrate the effectiveness of our new approach to eliminating residual azides from surface chemical functionalization by the Huisgen reaction.

CONCLUSIONS

In summary, we have successfully monitored surface Huisgen reactions between azide-terminated self-assembled monolayers and various alkynes by utilizing a combination of metal oxide nanowires and FT-IR spectroscopy. The time-dependent FT-IR spectrum showed that relatively concentrated Cu(I) catalysts (3.0 mM) and appropriate ligands are needed to obtain good conversion of the surface azides. At the same time, even under optimized conditions, the surface azides were not fully converted, in contrast to those in the solution. We found that this limitation is related to the proximity of surface azides on the SAM. We developed a mixed-SAM method to decrease the surface density of the reaction points and successfully improved the azide conversion rate to achieve almost stoichiometric conversion. These results demonstrate the effectiveness of our approach to providing stable azide-free interfaces by controlling the steric environment around the surface reaction points.

EXPERIMENTAL SECTION

Growth of ZnO Nanowires. ZnO nanowire arrays on Si (100) wafers were grown using the hydrothermal method. First, a 5 nm Ti buffer layer was sputtered onto the Si substrate (2 cm × 2.5 cm), and then a 100 nm ZnO film was sputtered on as the seed layer. Zinc nitrate hexahydrate (25 mM, $Zn(NO_3)_2{\cdot}6H_2O$, 99.0%), 25 mM hexamethylenetetramine (HMTA, $(CH_2)_6N_4$, 99.0%), and 2.5 mM polyethyleneimine (PEI, M_w 1800, 50 wt % in H_2O) were dissolved sequentially in deionized (DI) water (200 mL). The pre-prepared substrate was dipped into the solution and maintained at 80 °C for 24 h. After growth, the samples were rinsed with DI water and dried under N_2 flow. Then the as-grown ZnO nanowires were annealed at 400 °C in air for 1 h.

Characterization of ZnO Nanowires Morphology. Scanning electron microscope (SEM) images were acquired using a JEOL JSM-7610F instrument. The SEM images (Figure S1) confirm that the grown ZnO nanowires exhibit hexagonal columnar structures (diameter of ∼100 nm), which indicates that the ZnO nanowires have a single wurtzite structure with the prism (10−10) plane as the main face.

https://doi.org/10.1021/acs.langmuir.1c00106
Langmuir 2021, 37, 5172−5179

Table 2. Scope of Alkynes[a]

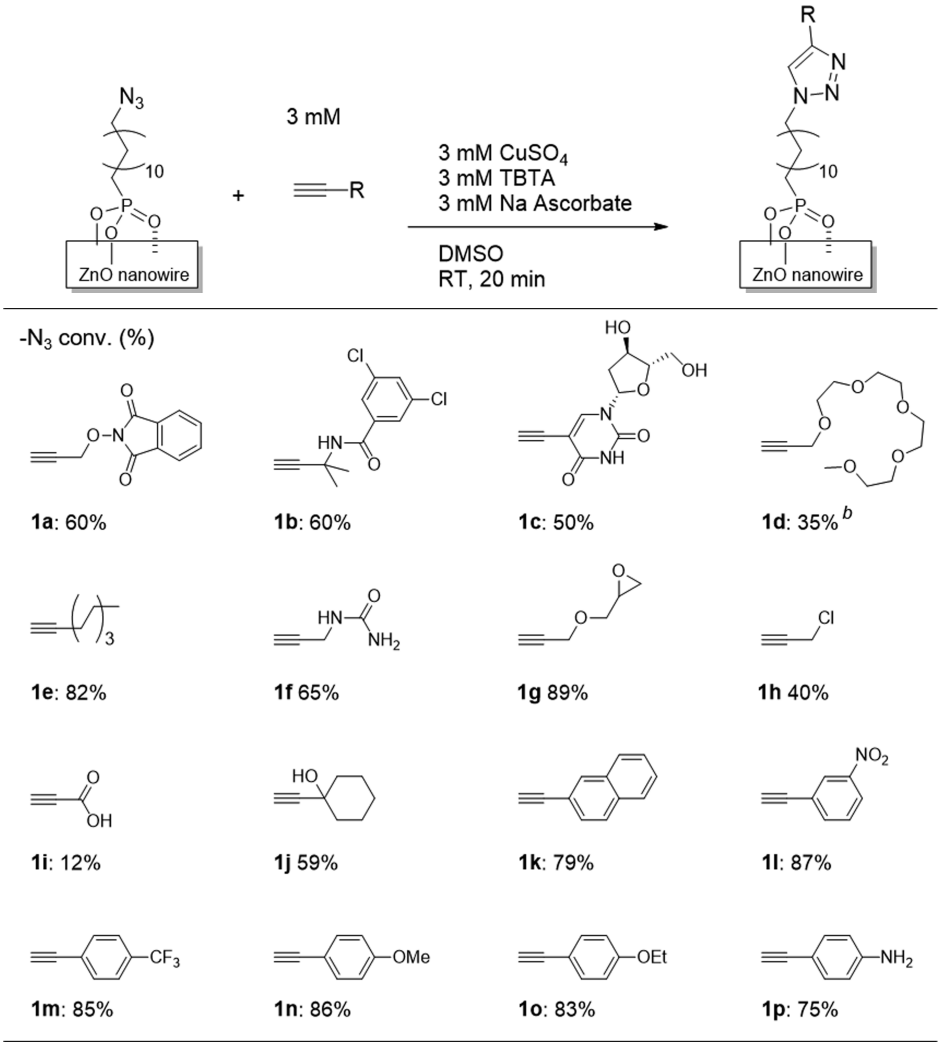

[a]The common reaction condition for all alkynes is shown on the table. See the Supporting Information for the raw data of the IR spectral change of each alkyne. [b]Results of 5-min reaction.

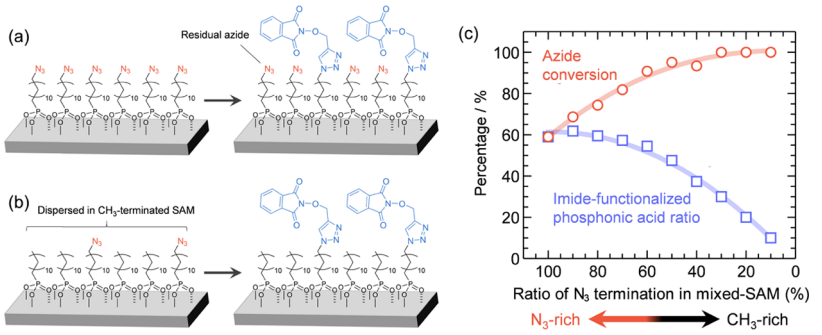

Figure 4. Effect of mixed-SAM on the azide reaction efficiency. (a) Click reaction on the pure azide-terminated SAM. (b) Click reaction on a mixed-SAM surface in which azide-terminated phosphonic acids are dispersed in methyl-terminated phosphonic acids. (c) Transformed N_3 ratio for initial N_3 amount on the SAM (red marks), and ratio of imide-functionalized molecules for all phosphonic acid molecules (blue marks) plotted against ratio of N_3 terminated phosphonic acid in the mixed-SAM.

Synthesis of (12-Azidododecyl)Phosphonic Acid. (12-azidododecyl)phosphonic acid was synthesized by a two-step reaction from 12-dibromododecane according to the literature procedure.[34]

Modification of (12-Azidododecyl)Phosphonic Acid SAM on ZnO Nanowires. Modification solutions (1.0 mM) were prepared by dissolving (12-azidododecyl)phosphonic acid in tetrahydrofuran at room temperature. The annealed ZnO nanowire array was dipped into the solution (10 mL) for 30 min at room temperature. Then, the samples were washed several times with tetrahydrofuran and dried under N_2 flow.

Huisgen Cycloaddition on SAM-Modified ZnO Nanowires. A reaction mixture for surface Huisgen cycloaddition was prepared by

https://doi.org/10.1021/acs.langmuir.1c00106
Langmuir 2021, 37, 5172−5179

dissolving 3.0 mM each of copper(II) sulfate ($CuSO_4$, Wako, 97.5%), ligand (MBTA, BBTA, or TBTA), and sodium ascorbate into 20 mL of DMSO/H_2O (9/1), followed by addition of 3.0 mM of substrate alkyne. The SAM-modified ZnO nanowire array was dipped into the solution (10 mL) at room temperature for a given time. The samples were washed several times with tetrahydrofuran before the FT-IR and pMAIRS measurements.

FT-IR and pMAIRS Analysis of the Molecular Modification. The FT-IR and pMAIRS spectra of the surface molecules on the ZnO nanowires were recorded at room temperature on a Thermo Fisher Scientific Nicolet iS50 FT-IR spectrometer equipped with a mercury−cadmium−telluride (MCT) detector. 300 scans were accumulated to obtain each spectrum. For each pMAIRS measurement, a series of eight single-beam sample measurements were carried out at angles of incidence from 9 to 44° at 5° steps and with a resolution of 4 cm^{-1}. The test room was always purged with dry air. After collection of the sample data, the OP and IP spectra were automatically calculated with the pMAIRS software (Thermo Fisher Scientific). The theoretical details of the IR pMAIRS analysis can be found in the literature.[35−37] FT-IR and pMAIRS spectra for a bare ZnO was used as the background spectrum for the other measurements. Conversions of Huisgen cycloaddition were calculated as the ratio IR peak area against initial azide peak area. The each azide peak area was calibrated by the peak area of asymmetric vibration band of $-CH_2$. Yields of Huisgen cycloaddition were also calculated as the ratio IR peak area against initial azide peak area, after collecting IR calibration curve of **1a** by using known amount of **1a** solution drops with known concentrations.

Temperature-Dependent FT-IR Analyses on the SAM-Modified ZnO Nanowires. (12-azidodecyl)phosphonic acid-modified ZnO nanowires were placed in an electric furnace. The temperature in the furnace was increased linearly to a determined temperature (50, 75, 100, 125, 150, 175, 200, 225, 250, 275, 300, 325, or 350 °C) for 30 min. After the temperature reached to the determined value, the furnace temperature was kept at that temperature for 10 min. Then, the furnace temperature was allowed to cool down to room temperature. The FT-IR measurements were performed according to the procedure described above. The percentage of remaining azide was calculated as the azide peak ratio of after/before heating.

■ ASSOCIATED CONTENT

Supporting Information

The Supporting Information is available free of charge at https://pubs.acs.org/doi/10.1021/acs.langmuir.1c00106.

SEM images of ZnO nanowires; FT-IR spectral changes during Huisgen cycloadditions in various solvents; FT-IR spectra for the Huisgen cycloadditions with various alkynes (PDF)

■ AUTHOR INFORMATION

Corresponding Authors

Takuro Hosomi − *Department of Applied Chemistry, Graduate School of Engineering, The University of Tokyo, Tokyo 113-8656, Japan; Japan Science and Technology Agency (JST), PRESTO, Kawaguchi, Saitama 332-0012, Japan;* orcid.org/0000-0002-5649-6696; Phone: +81-3-5841-3840; Email: t-hosomi@g.ecc.u-tokyo.ac.jp

Takeshi Yanagida − *Department of Applied Chemistry, Graduate School of Engineering, The University of Tokyo, Tokyo 113-8656, Japan; Institute for Materials Chemistry and Engineering, Kyushu University, Kasuga, Fukuoka 816-8580, Japan;* orcid.org/0000-0003-4837-5701; Phone: +81-3-5841-3862; Email: yanagida@g.ecc.u-tokyo.ac.jp

Authors

Rimon Yamaguchi − *Department of Applied Chemistry, Graduate School of Engineering, The University of Tokyo, Tokyo 113-8656, Japan; Institute for Materials Chemistry and Engineering, Kyushu University, Kasuga, Fukuoka 816-8580, Japan*

Masaya Otani − *Department of Basic Science, Graduate School of Art and Sciences, The University of Tokyo, Tokyo 153-8902, Japan*

Kazuki Nagashima − *Department of Applied Chemistry, Graduate School of Engineering, The University of Tokyo, Tokyo 113-8656, Japan; Japan Science and Technology Agency (JST), PRESTO, Kawaguchi, Saitama 332-0012, Japan;* orcid.org/0000-0003-0180-816X

Tsunaki Takahashi − *Department of Applied Chemistry, Graduate School of Engineering, The University of Tokyo, Tokyo 113-8656, Japan; Japan Science and Technology Agency (JST), PRESTO, Kawaguchi, Saitama 332-0012, Japan;* orcid.org/0000-0002-2840-8038

Guozhu Zhang − *Department of Applied Chemistry, Graduate School of Engineering, The University of Tokyo, Tokyo 113-8656, Japan*

Masaki Kanai − *Institute for Materials Chemistry and Engineering, Kyushu University, Kasuga, Fukuoka 816-8580, Japan*

Hiroshi Masai − *Department of Basic Science, Graduate School of Art and Sciences, The University of Tokyo, Tokyo 153-8902, Japan*

Jun Terao − *Department of Basic Science, Graduate School of Art and Sciences, The University of Tokyo, Tokyo 153-8902, Japan;* orcid.org/0000-0003-1867-791X

Complete contact information is available at: https://pubs.acs.org/10.1021/acs.langmuir.1c00106

Author Contributions

Sample fabrication, spectroscopic measurements, and sensor evaluations were performed by R.Y. Characterizations of the nanowire and molecular functionalization states by the obtained data were conducted by R.Y., T.H., K.N., T.T., and T.Y. (12-azidododecyl)phosphonic acid was synthesized by M.O., H.M., and J.T. The surface reaction behaviors were discussed by R.Y., T.H., K.N., T.T., G.Z., M.K., M.O., H.M., J.T., and T.Y. This manuscript was written by T.H. and T.Y., while R.Y., K.N., T.T., G.Z., M.K., M.O., H.M., and J.T. contributed improvements. All the authors contributed to the manuscript preparation and approved the final version of the manuscript.

Notes

The authors declare no competing financial interest.

■ ACKNOWLEDGMENTS

This work was supported by KAKENHI (Grant Nos. JP20H02, JP18H01831, JP18H05243, and JP18KK0112). T.H. was supported by JST PRESTO, Japan (Grant No. JPMJPR19T8). T.H., K.N., T.T., and T.Y. were supported by JST CREST, Japan (Grant No. JPMJCR19I2), JST Mirai R&D. T.Y. and K.N. were supported by the CAS-JSPS Joint Research Projects (Grant No. JPJSBP120187207). This work was performed under the Cooperative Research Program of the Network Joint Research Center for Materials and Devices, the Dynamic Alliance for Open Innovation Bridging Human,

Environment and Materials, and the MEXT project "Integrated Research Consortium on Chemical Sciences".

REFERENCES

(1) Schoenbaum, C. A.; Schwartz, D. K.; Medlin, J. W. Controlling the Surface Environment of Heterogeneous Catalysts Using Self-Assembled Monolayers. *Acc. Chem. Res.* **2014**, *47*, 1438−1445.
(2) Vutti, S.; Schoffelen, S.; Bolinsson, J.; Buch-Månson, N.; Bovet, N.; Nygård, J.; Martinez, K. L.; Meldal, M. Click Chemistry Mediated Functionalization of Vertical Nanowires for Biological Applications. *Chem. − Eur. J.* **2016**, *22*, 496−500.
(3) He, C.; Abraham, B.; Fan, H.; Harmer, R.; Li, Z.; Galoppini, E.; Gundlach, L.; Teplyakov, A. V. Morphology-Preserving Sensitization of ZnO Nanorod Surfaces via Click-Chemistry. *J. Phys. Chem. Lett.* **2018**, *9*, 768−772.
(4) Kantheti, S.; Narayan, R.; Raju, K. V. Pyrene-Anchored ZnO Nanoparticles through Click Reaction for the Development of Antimicrobial and Fluorescent Polyurethane Nanocomposite. *Polym. Int.* **2015**, *64*, 267−274.
(5) Haensch, C.; Hoeppener, S.; Schubert, U. S. Chemical Modification of Self-Assembled Silane Based Monolayers by Surface Reactions. *Chem. Soc. Rev.* **2010**, *39*, 2323−2334.
(6) Shah, S.; Benson, M. C.; Bishop, L. M.; Huhn, A. M.; Ruther, R. E.; Yeager, J. C.; Tan, Y.; Louis, K. M.; Hamers, R. J. Chemically Assembled Heterojunctions of SnO_2 Nanorods with TiO_2 Nanoparticles via "Click" Chemistry. *J. Mater. Chem.* **2012**, *22*, 11561−11567.
(7) Mehlich, J.; Ravoo, B. J. Click Chemistry by Microcontact Printing on Self-Assembled Monolayers: A Structure-Reactivity Study by Fluorescence Microscopy. *Org. Biomol. Chem.* **2011**, *9*, 4108−4115.
(8) Rozkiewicz, D. I.; Gierlich, J.; Burley, G. A.; Gutsmiedl, K.; Carell, T.; Ravoo, B. J.; Reinhoudt, D. N. Transfer Printing of DNA by "Click" Chemistry. *ChemBioChem* **2007**, *8*, 1997−2002.
(9) Michel, O.; Ravoo, B. J. Carbohydrate Microarrays by Microcontact "Click" Chemistry. *Langmuir* **2008**, *24*, 12116−12118.
(10) Godula, K.; Rabuka, D.; Nam, K. T.; Bertozzi, C. R. Synthesis and Microcontact Printing of Dual End-Functionalized Mucin-like Glycopolymers for Microarray Applications. *Angew. Chem., Int. Ed.* **2009**, *48*, 4973−4976.
(11) Poonthiyil, V.; Lindhorst, T. K.; Golovko, V. B.; Fairbanks, A. J. Recent Applications of Click Chemistry for the Functionalization of Gold Nanoparticles and Their Conversion to Glyco-Gold Nanoparticles. *Beilstein J. Org. Chem.* **2018**, *14*, 11−24.
(12) Amblard, F.; Cho, J. H.; Schinazi, R. F. Cu(I)-Catalyzed Huisgen Azide−Alkyne 1,3-Dipolar Cycloaddition Reaction in Nucleoside, Nucleotide, and Oligonucleotide Chemistry. *Chem. Rev.* **2009**, *109*, 4207−4220.
(13) Bandyopadhyay, S.; Mukherjee, S.; Dey, A. Modular Synthesis, Spectroscopic Characterization and in Situ Functionalization Using "Click" Chemistry of Azide Terminated Amide Containing Self-Assembled Monolayers. *RSC Adv.* **2013**, *3*, 17174−17187.
(14) Xi, W.; Scott, T. F.; Kloxin, C. J.; Bowman, C. N. Click Chemistry in Materials Science. *Adv. Funct. Mater.* **2014**, *24*, 2572−2590.
(15) Collman, J. P.; Devaraj, N. K.; Eberspacher, T. P. A.; Chidsey, C. E. D. Mixed Azide-Terminated Monolayers: A Platform for Modifying Electrode Surfaces. *Langmuir* **2006**, *22*, 2457−2464.
(16) Fryxell, G. E.; Rieke, P. C.; Wood, L. L.; Engelhard, M. H.; Williford, R. E.; Graff, G. L.; Campbell, A. A.; Wiacek, R. J.; Lee, L.; Halverson, A. Nucleophilic Displacements in Mixed Self-Assembled Monolayers. *Langmuir* **1996**, *12*, 5064−5075.
(17) Deckert, A. A.; Lesko, J.; Todaro, S.; Doyle, M.; Delaney, C. Kinetics and Mechanism of Substitution Reactions between Myoglobin and Activated Self-Assembled Monolayers Investigated Using Surface Plasmon Resonance. *Langmuir* **2002**, *18*, 8156−8160.
(18) Choi, I. S.; Chi, Y. S. Surface Reactions On Demand: Electrochemical Control of SAM-Based Reactions. *Angew. Chem., Int. Ed.* **2006**, *45*, 4894−4897.
(19) Al-Hajj, N.; Mousli, Y.; Miche, A.; Humblot, V.; Hunel, J.; Heuzé, K.; Buffeteau, T.; Genin, E.; Vellutini, L. Influence of the Grafting Process on the Orientation and the Reactivity of Azide-Terminated Monolayers onto Silica Surface. *Appl. Surf. Sci.* **2020**, *527*, No. 146778.
(20) Bishop, L. M.; Yeager, J. C.; Chen, X.; Wheeler, J. N.; Torelli, M. D.; Benson, M. C.; Burke, S. D.; Pedersen, J. A.; Hamers, R. J. A Citric Acid-Derived Ligand for Modular Functionalization of Metal Oxide Surfaces via "Click" Chemistry. *Langmuir* **2012**, *28*, 1322−1329.
(21) Henriksson, A.; Friedbacher, G.; Hoffmann, H. Surface Modification of Silicon Nanowires via Copper-Free Click Chemistry. *Langmuir* **2011**, *27*, 7345−7348.
(22) Wang, C.; Hosomi, T.; Nagashima, K.; Takahashi, T.; Zhang, G.; Kanai, M.; Zeng, H.; Mizukami, W.; Shioya, N.; Shimoaka, T.; Tamaoka, T.; Yoshida, H.; Takeda, S.; Yasui, T.; Baba, Y.; Aoki, Y.; Terao, J.; Hasegawa, T.; Yanagida, T. Rational Method of Monitoring Molecular Transformations on Metal-Oxide Nanowire Surfaces. *Nano Lett.* **2019**, *19*, 2443−2449.
(23) Wang, C.; Hosomi, T.; Nagashima, K.; Takahashi, T.; Zhang, G.; Kanai, M.; Yoshida, H.; Yanagida, T. Phosphonic Acid Modified ZnO Nanowire Sensors: Directing Reaction Pathway of Volatile Carbonyl Compounds. *ACS Appl. Mater. Interfaces* **2020**, *12*, 44265−44272.
(24) Hotchkiss, P. J.; Malicki, M.; Giordano, A. J.; Armstrong, N. R.; Marder, S. R. Characterization of Phosphonic Acid Binding to Zinc Oxide. *J. Mater. Chem.* **2011**, *21*, 3107−3112.
(25) Schulmeyer, T.; Paniagua, S. A.; Veneman, P. A.; Jones, S. C.; Hotchkiss, P. J.; Mudalige, A.; Pemberton, J. E.; Marder, S. R.; Armstrong, N. R. Modification of BaTiO3 Thin Films: Adjustment of the Effective Surface Work Function. *J. Mater. Chem.* **2007**, *17*, 4563−4570.
(26) Timpel, M.; Nardi, M. V.; Krause, S.; Ligorio, G.; Christodoulou, C.; Pasquali, L.; Giglia, A.; Frisch, J.; Wegner, B.; Moras, P.; Koch, N. Surface Modification of ZnO(0001)−Zn with Phosphonate-Based Self-Assembled Monolayers: Binding Modes, Orientation, and Work Function. *Chem. Mater.* **2014**, *26*, 5042−5050.
(27) Quiñones, R.; Shoup, D.; Behnke, G.; Peck, C.; Agarwal, S.; Gupta, R. K.; Fagan, J. W.; Mueller, K. T.; Iuliucci, R. J.; Wang, Q. Study of Perfluorophosphonic Acid Surface Modifications on Zinc Oxide Nanoparticles. *Materials* **2017**, *10*, No. 1363.
(28) Hasegawa, T.; Iiduka, Y.; Kakuda, H.; Okada, T. Analysis of Structurally Heterogeneous Langmuir-Blodgett Films of Folded/Unfolded Long-Chain Molecules by Infrared Multiple-Angle Incidence Resolution Spectroscopy. *Anal. Chem.* **2006**, *78*, 6121−6125.
(29) Yoffe, A. D. Thermal Decomposition and Explosion of Azides. *Proc. R. Soc. A* **1951**, *208*, 188−199.
(30) Valiokas, R.; Östblom, M.; Svedhem, S.; Svensson, S. C. T.; Liedberg, B. Thermal Stability of Self-Assembled Monolayers: Influence of Lateral Hydrogen Bonding. *J. Phys. Chem. B* **2002**, *106*, 10401−10409.
(31) Moses, J. E.; Moorhouse, A. D. The Growing Applications of Click Chemistry. *Chem. Soc. Rev.* **2007**, *36*, 1249−1262.
(32) Hein, J. E.; Fokin, V. V. Copper-Catalyzed Azide-Alkyne Cycloaddition (CuAAC) and beyond: New Reactivity of Copper(I) Acetylides. *Chem. Soc. Rev.* **2010**, *39*, 1302−1315.
(33) Chan, T. R.; Hilgraf, R.; Sharpless, K. B.; Fokin, V. V. Polytriazoles as Copper(I)-Stabilizing Ligands in Catalysis. *Org. Lett.* **2004**, *6*, 2853−2855.
(34) Toulemon, D.; Pichon, B. P.; Leuvrey, C.; Zafeiratos, S.; Papaefthimiou, V.; Cattoën, X.; Bégin-Colin, S. Fast Assembling of Magnetic Iron Oxide Nanoparticles by Microwave-Assisted Copper-(I) Catalyzed Alkyne−Azide Cycloaddition (CuAAC). *Chem. Mater.* **2013**, *25*, 2849−2854.
(35) Hasegawa, T. A Novel Measurement Technique of Pure Out-of-Plane Vibrational Modes in Thin Films on a Nonmetallic Material with No Polarizer. *J. Phys. Chem. B* **2002**, *106*, 4112−4115.
(36) Itoh, Y.; Kasuya, A.; Hasegawa, T. Analytical Understanding of Multiple-Angle Incidence Resolution Spectrometry Based on a

https://doi.org/10.1021/acs.langmuir.1c00106
Langmuir 2021, 37, 5172−5179

Classical Electromagnetic Theory. *J. Phys. Chem. A* **2009**, *113*, 7810−7817.
(37) Shioya, N.; Shimoaka, T.; Murdey, R.; Hasegawa, T. Accurate Molecular Orientation Analysis Using Infrared P-Polarized Multiple-Angle Incidence Resolution Spectrometry (PMAIRS) Considering the Refractive Index of the Thin Film Sample. *Appl. Spectrosc.* **2017**, *71*, 1242−1248.

https://doi.org/10.1021/acs.langmuir.1c00106
Langmuir 2021, 37, 5172−5179